Synthesis and Characterization of Polyethylene-Octene Elastomer/Clay/Biodegradable Starch Nanocomposites

Hsin-Tzu Liao, Chin-San Wu

Department of Biochemical Engineering and Graduate Institute of Environmental Polymer Materials, Kao Yuan Institute of Technology, Kaohsiung County, Taiwan 82101, Republic of China

Received 20 April 2004; accepted 10 December 2004
DOI 10.1002/app.21763
Published online in Wiley InterScience (www.interscience.wiley.com).

ABSTRACT: The aim of this work is the production of new nanocomposites from metallocene polyethylene-octene elastomer (POE), montmorillonite and *biodegradable* starch by means of a melt blending method. Characterizations of clay, modified clay, POE, POE-g-AA, and the hybrids produced from polymer, clay, and/or starch were performed by X-ray diffraction (XRD) spectroscopy, Fourier transform infrared (FTIR) spectrophotometer, differential scanning calorimetry (DSC), thermogravimetry analyzer (TGA), scanning electron microscope (SEM), and Instron mechanical tester. As to the results, organophilic clay can be well dispersed into acrylic acid grafted polyethylene-octene elastomer (POE-g-AA) in nanoscale sizes since cetyl pyridium chloride is partially compatible with POE-g-AA and allows POE-g-AA chains to intercalate into clay layers. Based on consideration of thermal and mechanical properties, it is also found that 12 wt % of clay content is optimal for preparation of POE-g-AA/clay nanocomposites. The new *partly* biodegradable POE-g-AA/clay/starch hybrid could obviously improve the elongation and the tensile strength at break of the POE-g-AA/starch hybrid since the former can give the smaller starch phase size and nanoscale dispersion of silicate layers in the polymer matrix. The nanocomposites produced from our laboratory can provide a stable tensile strength at break when the starch content is up to 40 wt %. © 2005 Wiley Periodicals, Inc. J Appl Polym Sci 97: 397–404, 2005

Key words: polyethylene; octane; clay; surfactant

INTRODUCTION

Inorganic clay minerals, such as montmorillonite and hectrite, have been widely used as reinforcement materials for polymers due to their nanoscale size and intercalation properties.[1–3] In recent years, polymer/silicate hybrid nanocomposites have been of considerable interest as an effective method to develop new composite materials. There are two commercially attractive approaches, *in situ* polymerization and melt exfoliation, for preparing polymer/clay nanocomposites. The first method has been used for preparation of nylon 6-clay hybrid, and the results showed that strength, modulus, and heat distortion temperature of virgin nylon 6 could be increased markedly.[4–7] The melt intercalation method was first demonstrated by Vaia and coworkers,[2] and then it became a mainstream for the preparation of polymer/clay nanocomposites without *in situ* interactive polymerization, especially for the case of polyolefin-based nanocomposites.[8–12] There were some proposals for the preparation of polypropylene/clay and polyethylene/clay nanocomposites.[10–17] The effect of size and type of the clay minerals to the properties of polyimide/clay hybrids has been studied by Yano and colleagues.[18] In their study, hectrite, saponite, montmorillonite, and synthetic mica were used as clay minerals, and the results showed that the longer the length of clay mineral was, the more effectively properties of the polyimide were improved.

Polyethylene is one of the most widely used polyolefin polymers, but its use is restricted in certain applications by its low melting point, biodegradability, stability in hydrocarbons, and a tendency to crack when stressed. Research on graft reaction, crosslinking reaction, and blending with inorganic fillers for polyethylene, to mitigate its disadvantages, have been extensively investigated for many years. Recently, the metallocene based polyethylene-octene elastomer (POE), which is developed using a metallocene catalyst by Dow and Exxon, has received much attention due to its unique uniform distribution of comonomer content and narrow molecular weight distribution.[19,20] It seems that study on synthesis and characterization of POE/clay nanocomposites using the melt exfoliation method has not been found in our literature survey, though researches of PE/clay and PP/clay nanocomposites have been proposed in the past.

Since POE does not include any polar groups in its backbone, it is thought that homogeneous dispersion of the hydrophilic clay minerals in the hydrophobic POE matrix is not realized. In general, the clay is

Correspondence to: H.-T. Liao (htliaw@cc.kyit.edu.tw).

© 2005 Wiley Periodicals, Inc.

modified with alkylammonium to facilitate its interaction with a polymer because the alkylammonium makes the clay surface organophilic. To obtain good dispersion of the organically modified clay in nonpolar olefin polymers, a polar functional oligomer as a compatabilizer, such as maleic anhydride modified PP oligomers, may be used to approach this purpose since such nonpolar polymers are still too hydrophobic.[12,13,16,21,22] Though the POE itself was not biodegradable, a higher amount of biodegradable fillers incorporated with the polymer can reduce the amount of waste plastics and the cost of POE. Blending of POE with organic fillers, such as starch and wood flour, is of considerable interest in industry to improve its biodegradable property. In this study, starch was chosen as the organic filler because it is an abundant, inexpensive, renewable, and fully biodegradable natural raw material.

The purpose of this study was to prepare the *partly* biodegradable POE/clay/starch nanocomposites by the simple melt blending method to mitigate the disadvantages of POE. To obtain homogeneous dispersions of the clay minerals and the starch in the POE matrix, cetyl pyridium chloride (CPC) pretreated montmorillonite and acrylic acid grafted polyethylene-octene elastomer (POE-g-AA) are used as the organophilic clay and the polymer matrix, respectively. The effect of introducing clay and starch on the properties of hybrids is also investigated. The treated and untreated clays, pure POE, POE-g-AA, and hybrid products (POE/clay, POE-g-AA/clay, POE/starch, POE-g-AA/starch, and POE-g-AA/clay/starch) are characterized by Fourier transform infrared (FTIR) spectrophotometer, scanning electron microscope (SEM), and X-ray diffractometer (XRD). Moreover, the thermal and mechanical properties of hybrids are also examined by differential scanning calorimetry (DSC), thermogravimetry analyzer (TGA), and Instron mechanical tester.

EXPERIMENTAL

Materials

The POE copolymer with 18% octene (Engage 8003, Dow Chemical Corp., Wilminton, ED) and the montmorillonite with a cation-exchange capacity of 119 meq/100g ("Kunipia F", Kunimine Corp., Japan) were used as received. Acrylic acid (AA, Aldrich Chemical Corp., Milwaukee, WI) was purified by recrystallization from chloroform before use. The initiator dicumyl peroxide (DCP, Aldrich Chemical Corp., Milwaukee, WI) was recrystallized twice by dissolving in absolute methanol, filtering the solution while hot, and chilling in ice water. The starch (Sigma Chemical Corp., Steinheim, Germany) had compositions of 27% amylose and 73% amylopectine. The starch was cleaned with acetone and then dried in an oven at 105°C for 24 h prior to blending. Cetyl pyridium chloride (CPC, greater than 99% purity, Sigma Chemical Corp., Steinheim, Germany) was used as a cationic surfactant and without further purification. Other reagents were purified by the conventional methods. The POE-g-AA copolymer was made in our laboratory and its grafting percentage was about 5.65 wt %.

Samples preparation

POE-g-AA copolymer

The grafting reaction of AA onto molten POE was performed by using xylene as an interface agent and DCP as an initiator under a nitrogen atmosphere at 85 $\pm$ 2°C. The reaction lasted for 6 h with a rotor speed of 60 rpm. The grafting percentage was determined by a titration method,[23] and the result showed that it was about 5.65 wt % when DCP and AA loadings were kept at 0.3 wt % and 10 wt %, respectively. More information about the grafting reaction of AA onto POE can be referred to in our previous works.[24,25]

Preparation of organophilic clays

The preparation of modified clays was according to the method proposed by Tseng and coworkers.[1] In a 100 mL beaker, a sample of 1 g sodium montmorillonite was dissolved in 50 mL of distilled water under vigorous stirring, to form a uniformly dispersed solution, and then 0.40 g and 0.20 g of cetyl pyridium chloride were added to the solution for clay/CPC = 1/1 (clay-CPC) and clay/CPC = 1/0.5, respectively. The mixture was further stirred vigorously 8 h at room temperature and then filtered and washed with deionized water. The product was freeze-dried in a vacuum oven at room temperature for 24 h. The organophilic clay mineral thus obtained is highly hydrophobic.

Preparation of hybrids from POE, POE-g-AA, clay-CPC, and starch

The hybrids, including POE/clay-CPC, POE-g-AA/clay-CPC, POE/starch, POE-g-AA/starch, and POE-g-AA/clay-CPC/starch, were prepared by the melt blending method using a BRABENDER "PLATOGRAPH" 200 Nm MIXER W50EHT instrument (Duisburg, Germany). For the preparation of hybrids, the organically modified montmorillonite with clay/CPC = 1/1 was chosen as the reinforcement material. A determined amount of POE or POE-g-AA sample was put into the BRABENDER instrument with blade type rotor to melt it under the conditions of rotor speed and blending temperature at 50 rpm and 140 $\sim$ 150°C, respectively. When the POE or POE-g-AA had melted completely, preweighed amounts of the well-dried

clay-CPC and/or the starch were added into the MIXER for another 15 min to produce the hybrid. For POE/clay-CPC and POE-g-AA/clay-CPC hybrids, the mass ratios of clay-CPC to POE or POE-g-AA were chosen as 3/97, 6/94, 9/91, 12/88, 15/85, and 20/80. For preparation of *partly* biodegradable nanocomposites, the starch contents were 10, 20, 30, and 40 wt %, and the mass ratio of clay-CPC to POE-g-AA was kept constant at 12/88. The hybrid products were pressed into thin plates by a hot press at 140°C, and then they were put into a dryer for cooling. Next, the cool thin plates were made into standard specimens for characterization.

Characterizations of hybrids

XRD analysis

The X-ray diffraction patterns were recorded on the Rigaku D/max 3V X-ray diffractometer (Tokyo, Japan) using CuK-α radiation (wavelength, $\lambda = 0.1541$ nm) with a scanning rate of 2°/min, and the basal spacing of samples were determined from Bragg's law ($\lambda = 2d\sin\theta$).

FTIR analysis

A Fourier transform infrared spectrophotometer (Bio-Rad FTS-7PC type, Madison, WI), using thin films, was used to investigate the graft reaction of acrylic acid onto POE and to verify the incorporation of the modified clay to the extent that bonds were formed in the hybrids.

DSC analysis

The melting temperature (T_m) and the melting enthalpy (ΔH_m) of samples were determined from a differential scanning calorimeter (TA Instrument 2010 DSC system, New Castle, DE). For DSC tests, sample sizes ranged from 4 to 6 mg and the melting curves were taken at a temperature range of −30 to 120°C scanned at a heating rate of 10°C/min.

TGA analysis

The thermogravimetry analyzer (TA Instrument 2010 TGA system, New Castle, DE) was used to assess whether organic-inorganic phase interactions influenced the thermal degradation of the hybrids. Samples were placed in alumina crucibles and tested with a thermal ramp over the temperature range of 30 ~ 600°C at a heating rate of 20°C/min, and then the initial decomposition temperature (IDT) of the hybrids was obtained.

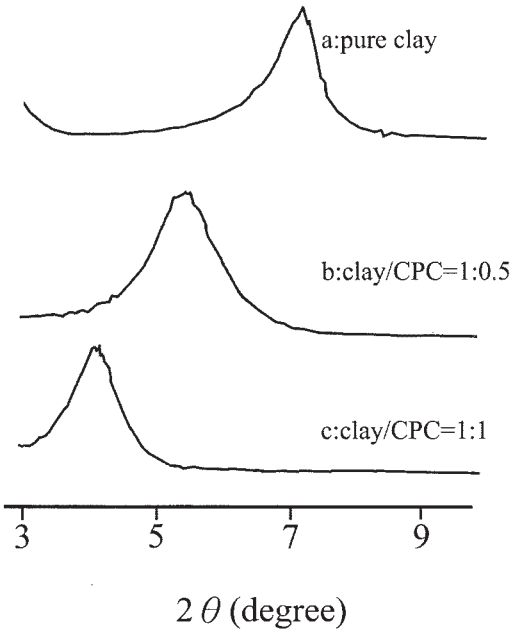

Figure 1 X-ray diffraction patterns ranging from $2\theta = 3°$ to 10° for pure and CPC treated clays.

SEM analysis

A scanning electron microscope (Hitachi microscope Model S-1400, Japan) was used to study the morphology of the hybrids and to measure the starch phase size in the polymers. Before the tests, the hybrid was prepared in a thin film by a hydrolytic press, and then the film was treated with hot water in 80°C for 24 h. Afterward, the films were coated with gold and observed by SEM.

Mechanical testing

According to the ASTM D638 method, the Instron mechanical tester (Model LLOYD, LR5K type) was used to measure the tensile strength and the elongation at break. The films of testing samples, which were conditioned at 50 ± 5% relative humidity for 24 h prior to the measurements, were prepared in a hydrolytic press at 140°C, and then the measurements were done using a 20 mm/min crosshead speed. Five measurements were performed for each sample, and the results were averaged to obtain a mean value.

RESULTS AND DISCUSSION

X-ray diffraction

The X-ray diffraction patterns ranging from $2\theta = 3$ to 9° for pure and CPC treated clays are illustrated in Figure 1a–c. For pure clay, Figure 1a, the XRD pattern shows a silicate (001) reflection at about $2\theta = 7.1°$ corresponding to a basal spacing of 1.24 nm. From

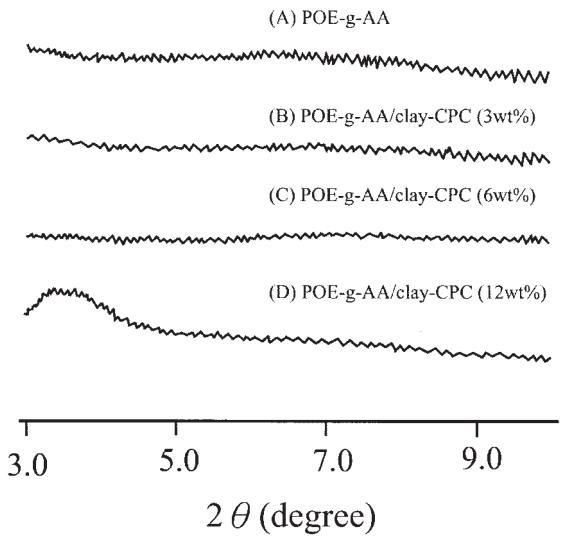

Figure 2 X-ray diffraction patterns ranging from $2\theta = 3°$ to 10° for (A) POE-g-AA, (B) POE-g-AA/clay-CPC (3 wt %), (C) POE-g-AA/clay-CPC (6 wt %), and (D) POE-g-AA/clay-CPC (12 wt %).

Figures 1b,c, it is clear that the CPC is indeed intercalated into the layers of clay since the layer spacing of clay is expanded by CPC. It is also found that the layer spacing of clay increases with an increasing of CPC content, where the basal spacing is increased to about 1.63 and 2.15 nm when the clay/CPC ratios are 1/0.5 and 1/1, respectively. This result is in agreement with the phenomenon proposed by Tseng and coworkers.[1] It is reasonable to assume that the presence of CPC is able to enhance the diffusion of the POE-g-AA chains into the silicate interlayers.

X-ray diffraction analysis was also used to study the dispersibility of clay in POE-g-AA/clay-CPC hybrids. The X-ray diffraction patterns proposed by Perez and colleagues[24] showed that there are two peaks at about $2\theta = 19.8°$ and $2\theta = 21.4°$ for pure POE. One peak ($2\theta = 21.4°$) reflects the characteristics of the orthorhombic cell of polyethylene, and the other peak ($2\theta = 19.8°$) may be considered as indicative of the side branches of octene in the crystalline structure. In our previous works,[25,26] there is only one peak at about $2\theta = 21.4°$ in the XRD pattern of the POE-g-AA copolymer. The disappearance of the peak at about $2\theta = 19.8°$ may be due to the change of coordination features of POE molecules when acrylic acid is grafted onto POE.

Figures 2A–D show the X-ray diffraction patterns ranging from $2\theta = 3$ to 10° for the POE-g-AA and the POE-g-AA/clay-CPC hybrids. As described above, it is clear that no reflection peak in the X-ray diffraction pattern ranging from $2\theta = 3$ to 10° can be observed for the POE-g-AA copolymer from Figure 2A. For the clay-CPC contents of 3 wt % and 6 wt %, as shown in Figures 2B,C, there is no apparent peak of clay that can be detected in the POE-g-AA/clay-CPC hybrids. This result indicates a homogeneous and fine dispersion of clay in the polymer matrix for low content of clay-CPC since the POE-g-AA chains can be intercalated into the narrow space of the CPC pretreated clay and then the clay has been exfoliated into larger than 10 nm thick layers with no regular repeated distance between layers. When the hybrid contains a larger amount of CPC pretreated clay, such as 12 wt %, the X-ray diffraction pattern of Figure 2D shows that a peak at about $2\theta = 3.5°$ can be observed. This peak, corresponding to the XRD pattern of pretreated clay with clay/CPC = 1/1 (Fig. 1D), reveals that the clay in the POE matrix is not well dispersed and indicates that some of the clay layers are not exfoliated.

Infrared spectroscopy

Figures 3A–D show the FTIR spectra of the pure POE, the POE-g-AA, a POE/clay-CPC (12 wt %) hybrid, and a POE-g-AA/clay-CPC (12 wt %) hybrid, respectively. As can be seen from Figure 3, all the characteristic peaks of POE at 2840–2928, 1465, and 720 cm^{-1} appear in the four polymers.[27,28] A comparison between Figure 3A,B shows that there are two extra peaks (1710 and 1247 cm^{-1}), which are the characteristic peaks of -C═O and -C-O, and a broad O-H stretching absorbance at about 3000–3600 cm^{-1} for the modified POE. Similar results can be found in some proposed articles.[27,29,30] So, one can confirm that acrylic acid has been successfully grafted onto POE chains since the discernible peaks near 1710 and 1247 cm^{-1}, based on free acid, appear in the spectrum of the modified POE. From Figures 3A,C, it can be seen that the FTIR spectrum of POE/clay-CPC (12 wt %) composite, as compared with that of the pure POE, shows new peaks at about 3600–3700 cm^{-1}, 1000–1100 cm^{-1}, and 400–500 cm^{-1}. The peak at about 3600–3700 cm^{-1} is due to the O-H bond stretching of the lattice water, and the peaks in the range of 1000–1100 cm^{-1} and 400–500 cm^{-1} indicate Si-O and Al-O stretching, and Si-O bending of the silicate phase. As a result, the interfacial force between the POE matrix and the clay layer is only established by the secondary valence force since no evidence of new absorption bands can be found in the spectrum, suggesting there are primary valence forces involved between POE and clay-CPC. A similar result can be found in some proposed papers.[31,32]

From Figures 3B,D, besides the common characteristic peaks of POE-g-AA, some extra peaks at 3600–3700 cm^{-1}, 1000–1100 cm^{-1}, 1100–1200 cm^{-1}, and 400–600 cm^{-1} appear in the spectrum of POE-g-AA/clay-CPC (12 wt %) hybrid. It has been shown that the peaks at about 3600–3700 cm^{-1}, 1000–1100 cm^{-1}, and 400–500 are due to the lattice water and the silicate phase. The peaks at 1100–1200 cm^{-1} indicate that the

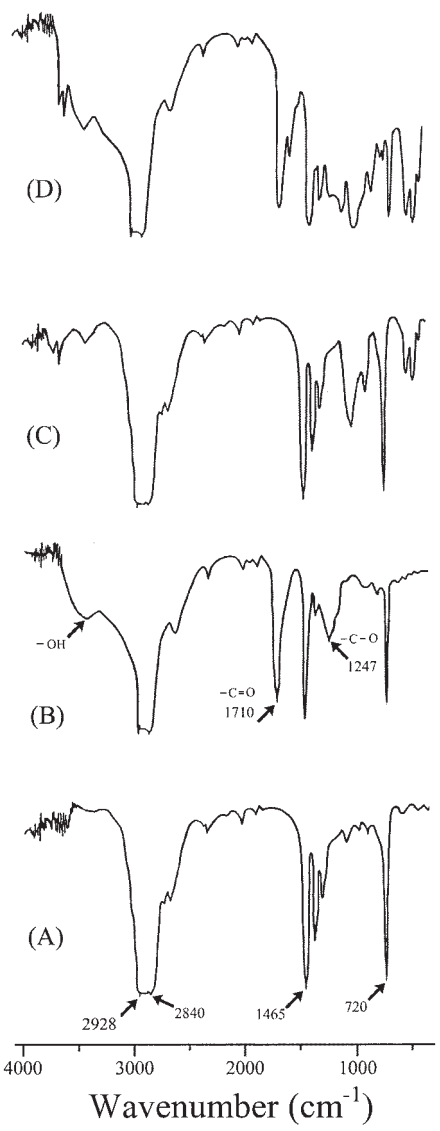

Figure 3 FTIR spectra of (A) pure POE, (B) POE-g-AA, (C) POE/clay-CPC (12 wt %), and (D) POE-g-AA/clay-CPC (12 wt %).

Si-O-C bond, which may be associated with an H-bonded Si-OH group, is produced from the reaction between POE-g-AA and the silicate phase of clay because absorbance of this covalent bond usually appears at 1080–1200 cm^{-1} (typically at 1080–1120 cm^{-1}).[28,33,34]

To understand the effect of starch on the *partly* biodegradable hybrids, the FTIR spectrophotometer was used to examine POE/starch (20 wt %), POE-g-AA/starch (20 wt %), and POE-g-AA/clay-CPC (9.6 wt %)/starch (20 wt %), and the results are illustrated in Figures 4A–C, respectively. In Figure 4, all the characteristic peaks of POE can be seen in the three polymers. A comparison of Figures 3A and 4A shows that there are two extra peaks, which are the characteristic peaks of the -C-O bond stretching vibration, at 1186 and 959 cm^{-1} in the FTIR spectrum of the POE/starch (20 wt %) blend.[35–37] It is also found that a broad O-H bond stretching in 3000–3600 cm^{-1} and a O-H bond bending at 1640 cm^{-1} appear in the FTIR spectrum of the POE/starch (20 wt %) blend. A similar result can be found in some proposed papers.[35,36] For the POE-g-AA/starch (20 wt %) (Fig. 4B), besides the common peaks appearing in the spectrum of the POE/starch (20 wt %) blend, there is a new absorption peak (at about 1739 cm^{-1}) corresponding to the ester carbonyl stretching vibration in the copolymer. According to the result proposed by Bikiaris and coworkers,[37] in which LDPE/plasticized starch blends were studied, the FTIR spectrum of ester carbonyl showed its functional group appeared at 1735 cm^{-1}. So, the appearance of this new absorption peak at about 1739 cm^{-1} may be due to the formation of an ester carbonyl functional group from the reaction between the -OH group of starch and the -COOH group of POE-g-AA. From Figures 4B,C, it can be seen that some extra peaks (3600–3700, 1100–1200, 1000–1100, and 400–

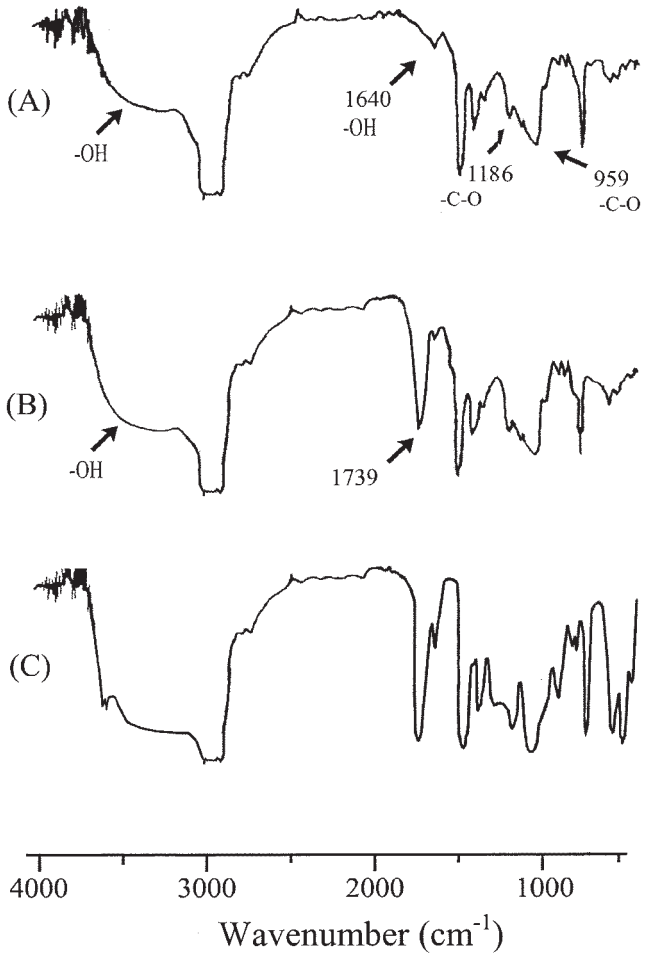

Figure 4 FTIR spectra of (A) POE/starch (20 wt %), (B) POE-g-AA/starch (20 wt %), (C) POE-g-AA/clay-CPC (9.6 wt %)/starch (20 wt %).

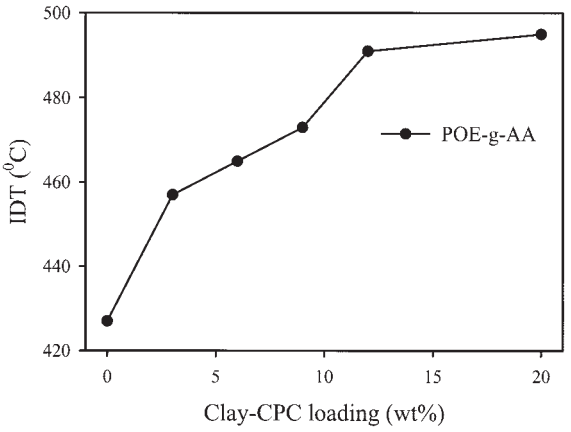

Figure 5 Initial decomposition temperature versus clay-CPC content for POE-g-AA/clay-CPC hybrids.

600 cm^{-1}) appear in the spectrum of the POE-g-AA/clay-CPC (9.6 wt %)/starch (20 wt %) hybrid. As discussed previously, those extra peaks are the consequence of the characteristic frequencies of clay and the formation of an Si-O-C bond. A similar result can be found in some proposed papers.[31,32]

Thermal stability of hybrids (DSC and TGA tests)

It is well known that the thermal stability of organic/inorganic hybrids depends on the interaction between the polymer chains and the inorganic network, and the consequential uniform distribution of the latter in the former matrix.[1,11] The variations of thermal property (initial decomposition temperature, IDT) with various clay-CPC contents were obtained from the TGA test for POE-g-AA/clay-CPC hybrids, and the results are illustrated in Figure 5. From Figure 5, it can be seen that the POE-g-AA/clay-CPC hybrids give a markedly positive effect on the value of IDT and the increment in IDT is about 70°C when the clay content is greater than 12 wt %. This result may be due to the nanoscale dispersion of clay and the formation of strong covalent Si-O-C bonds. Figure 5 also shows that the increment of IDT for POE-g-AA/clay-CPC hybrids is not significant when the clay content was greater than 12 wt %, since phase separation could occur in the hybrids for the clay content beyond this point.

The melting temperature (T_m) and the melting enthalpy (ΔH_m) of POE-g-AA/clay-CPC hybrids were obtained from the DSC test, and the results are summarized in Table I. As can be seen from Table I, the effect of clay loading on the melting temperature of POE-g-AA is fluctuant but slight. This result implies that the mean dimensions of the POE-g-AA crystals in the hybrids are not appreciably affected by the CPC treated montmorillonite particles. In contrast, substantially lower crystallinity (in terms of ΔH_m) for POE-g-AA/clay-CP hybrids is obtained. The decrease in the melting enthalpy for POE-g-AA can be associated with the increase in the clay content. This result is consistent with the data of other literature.[1,17]

TABLE I
Melting Temperature and Melting Enthalpy of POE-g-AA/Clay-CPC Nanocomposites at Different Clay-CPC Contents

Clay-CPC (wt %)	T_m (°C)	ΔH_m (J/g)
0	83.2	36.3
3	82.4	25.6
6	81.9	23.2
9	82.7	21.5
12	81.7	10.8
15	81.3	9.7

Mechanical properties of hybrids

The variation of tensile strength at break with clay-CPC content for POE-g-AA/clay-CPC hybrids is given in Figure 6. Similar to the effect of clay-CPC content on the thermal property, it can be seen from Figure 6 that the tensile strength of POE-g-AA/clay-CPC hybrids increases rapidly with the increasing of clay-CPC content from 0 to 12 wt % and then approaches a stable value. The positive effect on tensile strength may be due to the stiffness of the silicate layers contributing to the presence of immobilized or partially immobilized polymer phases[12] and to the nanoscale dispersion of silicate layers in the polymer matrix. It is also possible that silicate layer orientation as well as molecular orientation contribute to the observed reinforcement effect. The slight increment in tensile strength for the clay-CPC content above 12 wt % could be attributed to the inevitable aggregation of the clays in high clay content.

Figures 7 and 8 show the variations of elongation and tensile strength at break with the starch content

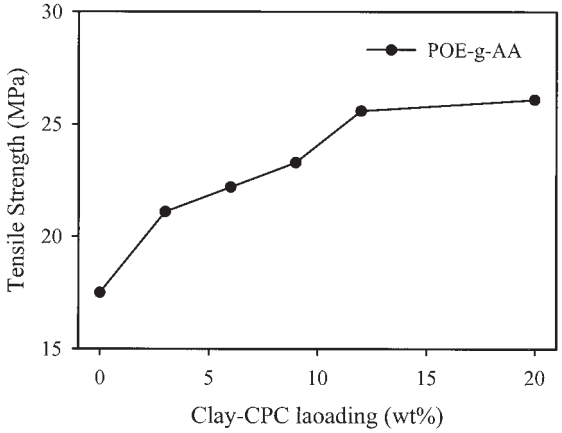

Figure 6 Tensile strength at break versus clay-CPC content for POE-g-AA/clay-CPC blends.

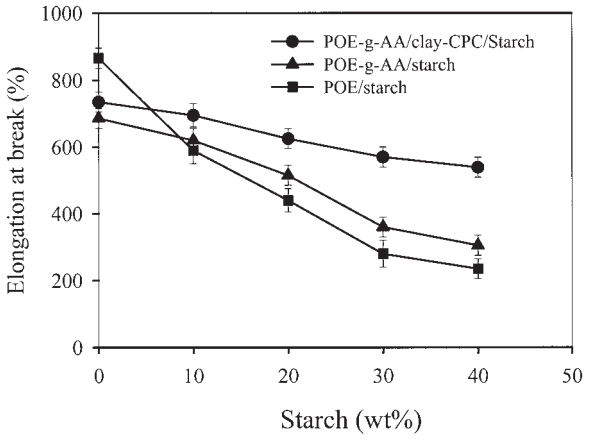

Figure 7 Elongation at break versus starch content for POE/starch, POE-g-AA/starch, and POE-g-AA/clay-CPC/starch hybrids.

for POE/starch, POE-g-AA/starch, and POE-g-AA/clay-CPC/starch blends. It can be seen that the tensile strength and the elongation of pure POE are both decreased when it is grafted with AA. To further understand the dispersibility of starch in these three blends with different starch content, the starch phase size was obtained from the SEM micrographs of the respective blends and the result is summarized in Table II. For POE/starch blends, both the elongation and the tensile strength at break decrease continuously and markedly from 870%/26.9Mpa to 220%/6.8Mpa as the starch content is increased from 0 to 40 wt % (the black solid square symbols in Figs. 7 and 8). Table II also shows that the starch phase size of POE/starch blends increases remarkably with an increasing of starch content. As might be expected, the POE/starch blends will give poor mechanical properties because of low adhesion and dispersivity between the two immiscible phases (hydrophobic POE and hydrophilic starch). It is evident that the mechanical properties strongly depend on the dispersion and the phase size of starch in the POE matrix because the larger starch phase size gives poorer adhesion and compatibility between starch and POE. So, the deterioration in mechanical properties of POE/starch blends can be explained from the phenomenon that the starch phase size of POE/starch blends increases with an increasing of starch content.

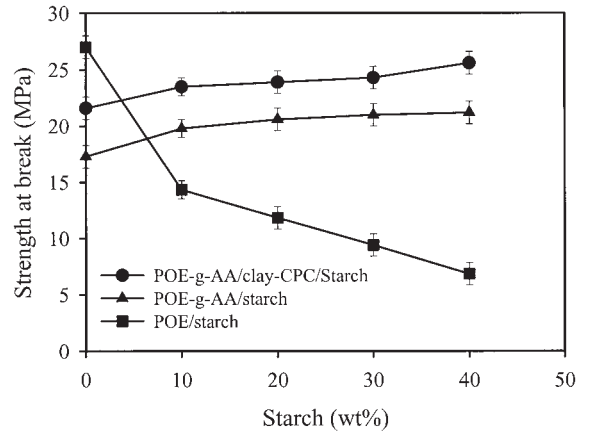

Figure 8 Tensile strength at break versus starch content for POE/starch, POE-g-AA/starch, and POE-g-AA/clay-CPC/starch hybrids.

TABLE II
The Starch Phase Size of POE/Starch, POE-g-AA/Starch, and POE-g-AA/Clay-CPC/Starch Blends at Different Starch Contents

Starch (wt %)	Phase size (μm)		
	POE/ Starch	POE-g-AA/ Starch	POE-g-AA/Clay-CPC/ Starch
10	4.5	1.5	0.8
20	8.0	2.0	1.0
30	12.5	3.0	1.5
40	16.0	3.5	1.8

For POE-g-AA/starch blends, as shown by the black solid triangular symbols in Figure 7, the elongation at break also decreases continuously with an increasing of the starch content, but they have larger values of elongation than those of the POE/starch blends. From the black solid triangular symbols in Figure 8, a quite different behavior of the tensile strength at break can be found, namely, the tensile strength at break of the POE-g-AA/starch blends increases with an increasing of starch content, although POE-g-AA has a lower value of tensile strength than that of the pure POE. It is also found that the POE-g-AA/starch blends not only give larger values of tensile strength than those of the POE/starch blends but also provide stable values of the tensile strength when the starch content is beyond 10 wt %. A contribution to this result may be the better dispersion and smaller phase size of starch in the POE-g-AA matrix (Table II). This better dispersion may arise from the formation of branched and crosslinked macromolecules, since this POE-g-AA copolymer has anhydride groups to react with the hydroxyls of starch. These macromolecules have higher tensile strength, compared to the linear ones, but lower elongation at break. Their presence could also explain, in part, why the increase in elongation at break was not as evident as in the tensile strength of the blends.

For POE-g-AA/clay-CPC/starch blends (the black solid circular symbols in Figs. 7 and 8), as compared to POE/starch and POE-g-AA/starch blends, much enhancement on the values of elongation and the tensile strength at break can be observed. The much better mechanical properties provided by the POE-g-AA/clay-CPC/starch blends may be coming from the much smaller starch phase size, the nanoscale disper-

sion of silicate layers in the polymer matrix, and the formation of the Si-O-C bond from the reaction between the POE-g-AA and the silicate phase of clay-CPC.

CONCLUSIONS

To enhance compatibility, thermal properties, and mechanical properties of POE/clay nanocomposites, the POE is modified with acrylic acid, and the clay minerals are pretreated by cetyl pyridium chloride before blending. From the X-ray diffraction patterns, it can be seen that the CPC can exfoliate the layer spacing of clay into the nanometer size and enhance the diffusion of the POE-g-AA chains into the silicate interlayers. The FTIR and XRD spectra prove that acrylic acid is really grafted onto the POE copolymer. TGA tests show that the POE-g-AA/clay-CPC hybrids could provide better thermal and mechanical properties than the POE/clay-CPC ones. These positive effects may be due to the stiffness of the silicate layers, the nanoscale dispersion of silicate layers in the polymer matrix (POE-g-AA), and the formation of the Si-O-C bond between POE-g-AA and the silicate phase of the clay-CPC. To improve the biodegradable property of the POE/clay hybrids, starch is chosen as the organic filler, and the results show that POE-g-AA/clay-CPC/starch hybrids could markedly improve the thermal and mechanical properties of POE/starch and POE-g-AA/starch hybrids since the nanoscale dispersion of silicate layers, the smallest starch phase size, and the primary valence forces can be obtained in the POE-g-AA/clay-CPC/starch hybrids. Finally, the *partly* biodegradable POE-g-AA/clay/starch nanocomposites produced from our laboratory can provide a stable tensile strength at break when the starch content is up to 40 wt %.

References

1. Tseng, C. R.; Wu, J. Y.; Lee, H. Y.; Chang, F. C. Polymer 2001, 42, 10063.
2. Vaia, R. A.; Ishii, H.; Giannelis, E. P. Chem Mater 1993, 5, 1694.
3. Okamoto, M.; Morita, S.; Kotaka, T. Polymer 2001, 42, 2685.
4. Usuki, A.; Kojima, Y.; Kawasumi, M.; Okada, A.; Fukushima, Y.; Kurauchi, T.; Kamigaito, O. J Mater Res 1993, 8, 1179.
5. Kojima, Y.; Usuki, A.; Kawasumi, M.; Okada, A.; Kurauchi, T.; Kamigaito, O. J Appl Polym Sci 1993, 49, 1259.
6. Murase, S.; Inoue, A.; Miyashita, Y.; Kimura, N.; Nishio, Y. J Polym Sci: Part B: Polym Phys 2002, 40, 479.
7. Kojima, Y.; Usuki, A.; Kawasumi, M.; Okada, A.; Fukushima, Y.; Kurauchi, T.; Kamigaito, O. J Mater Res 1993, 8, 1185.
8. Hasegawa, N.; Okamoto, H.; Kato, M.; Usuki, A. J Appl Polym Sci 2000, 78 1981.
9. Hasegawa, N.; Okamoto, H.; Kato, M.; Tsukigase, A.; Usuki, A. Macromol Mater Engng 2000, 280/281, 76.
10. Nam, P. H.; Maiti, P.; Okamoto, M.; Kotaka, T.; Hasegawa, N.; Usuki, A. Polymer 2001, 42, 9633.
11. Ma, J.; Qi, Z.; Hu, Y. J Appl Polym Sci 2001, 82, 3611.
12. Lin, X.; Wu, Q. Polymer 2001,42, 10013.
13. Wang, K. H.; Choi, M. H.; Koo, C. M.; Choi, Y. S.; Chung, I. J. Polymer 2001, 42, 9819.
14. Bergman, J. S.; Chen, H.; Giannelis, E. P.; Thomas, M. G.; Coates, G. W. Chem Commun 1999, 2179.
15. Yilgor, I.; Yilgor, E.; Suzer, S. J Appl Polym Sci 2002, 83, 1625.
16. Heinemann, J.; Reichert, P.; Thomann, R.; Mulhaupt, R. Macromol Rapid Commun 1999, 20, 423.
17. Privalko, E. G.; Pedoseuko, A. V.; Privalko, V. P.; Walt, R.; Friedrich, K. J Appl Polym Sci 1999, 73, 1267.
18. Yano, K.; Usuki, A.; Okada, A. J Polym Sci: Part A: Polym Chem 1997, 35, 2289.
19. Hwang, Y. C.; Chum, P. S.; Sehanobish, K. ANTEC 1994, 94, 3414.
20. Chum, P. S.; Kao, C. K.; Knight, G. W. Plastics Engineering June 1995, 21.
21. Teon, H. G.; Jung, H. T.; Lee, S. W.; Hudson, S. D. Polym Bull 1998, 41, 107.
22. Furuichi, N.; Kurokawa, Y.; Fujita, K.; Oya, A.; Yasuda, H.; Kiso, M. J Mater Sci 1996, 31, 4307.
23. Gaylord, N. G.; Mehta, R.; Kumar, V.; Tazi, M. J Appl Polym Sci 1989, 38, 359.
24. Perez, E.; Benavente, R.; Quijada, R.; Narvaez, A.; Galland, G. B. J Polym Sci, Part B: Polym Phys 2000, 38, 1440.
25. Wu, C. S.; Lai, S. M.; Liao, H. T. J Appl Polym Sci 2002, 85, 2905.
26. Wu, C. S.; Liao, H. T. J Appl Polym Sci 2002, 86, 1792.
27. Chandra, R.; Rustgi, R. Polym Degrad Stab 1997, 56, 185.
28. Breslin, V. T.; Li, B. J Appl Polym Sci 1993, 48 2063.
29. Fumihiko, M.; Shun, M.; Takshi, I. Polym J 1999, 31, 435.
30. Kim, J.; Tirrel, D. A. Macromol 1999, 32, 945.
31. Suga, K.; Rusling, J. F. Langmuir 1993, 9, 3649.
32. Lee, D. C.; Jang, L. W. J Appl Polym Sci 1996, 61, 1117.
33. Landry, C. J.; Coltrain, K.; Wesson, J. A.; Zumbulyadis, N.; Lippert, J. L. Polymer 1992, 33, 1496.
34. Zhou, W.; Dong, J. H.; Qiu, K. Y.; Wei, Y. J Appl Polym Sci 1998, 36, 1607.
35. Goheen, S. M.; Wool, R. P. J Appl Polym Sci 1991, 42, 2691.
36. Bikiaris, D.; Prinos, J.; Panayiotou, C. Polym Degrad Stab 1997, 56, 1.
37. Bikiaris, D.; Prinos, J.; Panayiotou, C. Polym Degrad Stab 1997, 58, 215.